

Enhanced ionic conductivity in LAGP/LATP composite electrolyte

Shi-Gang Ling(凌仕刚), Jia-Yue Peng(彭佳悦), Qi Yang(杨琪), Ji-Liang Qiu(邱纪亮), Jia-Ze Lu(卢嘉泽), Hong Li(李泓)
Citation: Chin. Phys. B . 2018, 27(3): 038201. **doi:** 10.1088/1674-1056/27/3/038201

Journal homepage: http://cpb.iphy.ac.cn; http://iopscience.iop.org/cpb

What follows is a list of articles you may be interested in

Gas treatment protection of metallic lithium anode

Wen-jun Li(李文俊), Quan Li(李泉), Jie Huang(黄杰), Jia-yue Peng(彭佳悦), Geng Chu(褚赓), Ya-xiang Lu(陆雅翔), Jie-yun Zheng(郑杰允), Hong Li(李泓)
Chin. Phys. B . 2017, 26(8): 088202. **doi:** 10.1088/1674-1056/26/8/088202

Conductivity and applications of Li-biphenyl-1, 2-dimethoxyethane solution for lithium ion batteries

Geng Chu(褚赓), Bo-Nan Liu(刘柏男), Fei Luo(罗飞), Wen-Jun Li(李文俊), Hao Lu(陆浩), Li-Quan Chen(陈立泉), Hong Li(李泓)
Chin. Phys. B . 2017, 26(7): 078201. **doi:** 10.1088/1674-1056/26/7/078201

A low cost composite quasi-solid electrolyte of LATP, TEGDME, and LiTFSI for rechargeable lithium batteries

Jie Huang(黄杰), Jia-Yue Peng(彭佳悦), Shi-Gang Ling(凌仕刚), Qi Yang(杨琪), Ji-Liang Qiu(邱纪亮), Jia-Ze Lu(卢嘉泽), Jie-Yun Zheng(郑杰允), Hong Li(李泓), Li-Quan Chen(陈立泉)
Chin. Phys. B . 2017, 26(6): 068201. **doi:** 10.1088/1674-1056/26/6/068201

Novel Fe_3O_4@SiO_2@Ag@Ni trepang-like nanocomposites: High-efficiency and magnetic recyclable catalysts for organic dye degradation

Chao Li(李超), Jun-Jie Sun(孙俊杰), Duo Chen(陈铎), Guang-Bing Han(韩广兵), Shu-Yun Yu(于淑云), Shi-Shou Kang(康仕寿), Liang-Mo Mei(梅良模)
Chin. Phys. B . 2016, 25(8): 088201. **doi:** 10.1088/1674-1056/25/8/088201

Nonlinear dynamic characteristics and optimal control of a giant magnetostrictive film-shaped memory alloy composite plate subjected to in-plane stochastic excitation

Zhu Zhi-Wen, Zhang Qing-Xin, Xu Jia
Chin. Phys. B . 2014, 23(8): 088201. **doi:** 10.1088/1674-1056/23/8/088201

Enhanced ionic conductivity in LAGP/LATP composite electrolyte*

Shi-Gang Ling(凌仕刚)[1,2], Jia-Yue Peng(彭佳悦)[1,2], Qi Yang(杨琪)[1,2], Ji-Liang Qiu(邱纪亮)[1,2], Jia-Ze Lu(卢嘉泽)[1,2], and Hong Li(李泓)[1,2,†]

[1] *Beijing National Laboratory for Condensed Matter Physics, Institute of Physics, Chinese Academy of Sciences, Beijing* 100190, *China*
[2] *University of Chinese Academy of Sciences, Beijing* 100049, *China*

(Received 10 October 2017; revised manuscript received 29 December 2017; published online 11 February 2018)

Nasicon materials (sodium superionic conductors) such as $Li_{1.5}Al_{0.5}Ge_{1.5}(PO_4)_3$ (LAGP) and $Li_{1.4}Al_{0.4}Ti_{1.6}(PO_4)_3$ (LATP) have been considered as important solid electrolytes due to their high ionic conductivity and chemical stability. Compared to LAGP, LATP has higher bulk conductivity around 10^{-3} S/cm at room temperature; however, the apparent grain boundary conductivity is almost two orders of magnitude lower than the bulk, while LAGP has similar bulk and grain boundary conductivity around the order of 10^{-4} S/cm. To make full use of the advantages of the two electrolytes, pure phase $Li_{1.5}Al_{0.5}Ge_{1.5}(PO_4)_3$ and $Li_{1.4}Al_{0.4}Ti_{1.6}(PO_4)_3$ were synthesized through solid state reaction, a series of composite electrolytes consisting of LAGP and LATP with different weight ratios were designed. XRD and variable temperature AC impedance spectra were carried out to clarify the crystal structure and the ion transport properties of the composite electrolytes. The results indicate that the composite electrolyte with the LATP/LAGP weight ratio of 80:20 achieved the highest bulk conductivity which shall be due to the formation of solid solution phase $Li_{1.42}Al_{0.42}Ge_{0.3}Ti_{1.28}(PO_4)_3$, while the highest grain boundary conductivity appeared at the LATP/LAGP weight ratio of 20:80 which may be due to the excellent interfacial phase between $Li_{1+x}Al_xGe_yTi_{2-x-y}(PO_4)_3$/LATP. All the composite electrolytes demonstrated higher total conductivity than the pure LAGP and LATP, which highlights the importance of heterogeneous interface on regulating the ion transport properties.

Keywords: solid electrolyte, composite, heterogeneous interface, enhanced conductivity

PACS: 82.47.Aa, 66.30.–h **DOI:** 10.1088/1674-1056/27/3/038201

1. Introduction

Lithium ion batteries have been widely used. All kinds of applications require high safety and high energy density. The electrolytes used in current commercial lithium ion batteries are flammable organic liquid electrolytes, which leads to thermal runaway. To enhance the safety and further improve the energy density of lithium batteries, researchers have paid wide attention to develop the solid state electrolyte which could be inflammable and compatible with the Li-contained high capacity anode.[1,2]

Generally, the solid state electrolytes are divided into two types. One is the polymer electrolyte, which uses the polymer molecular like polyethylene oxide (PEO), polyvinyliene fluoride (PVDF), polymethyl methacrylate (PMMA), polyacrylonitrile (PAN), polysiloxane, and so on, as the skeleton materials to cooperate with the lithium salt forming the dry polymer electrolyte.[3] These polymer electrolytes usually have low room temperature ionic conductivity in the vicinity of 10^{-6} S/cm, which is nearly three orders of magnitude lower than that of the liquid electrolytes and could not satisfy the kinetic demands of real applications in ambient surroundings. The other is the inorganic solid state electrolyte, mainly including sulfide and oxide compounds.[4] Usually, the sulfide electrolyte has higher ambient ionic conductivity than the oxide electrolyte, however, most sulfide electrolytes are not stable in the air and the chemical stability is relatively poor.[5] Compared to the sulfide electrolyte, the solid oxide electrolyte has better chemical and electrochemical stability. Some of them have acceptable room temperature ionic conductivity. The most interesting materials are garnet structure $Li_7La_3Zr_2O_{12}$ (LLZO),[6] perovskite structure $Li_{0.5}La_{0.5}TiO_3$ (LLTO),[7] LISICON structure $Li_{14}Zn(GeO_4)_4$ (LZGO),[8] NASICON structure $Li_{1.5}Al_{0.5}Ge_{1.5}(PO_4)_3$ (LAGP),[9] $Li_{1.4}Al_{0.4}Ti_{1.6}(PO_4)_3$ (LATP), and so on.[10,11]

Compared to LAGP and LATP, LLZO and LLTO contain rare earth elements, which could be costly. Besides, LLZO is not very stable in moist air while LLTO has a large grain boundary resistance.[12] The LISICON type LZGO has very low room temperature ionic conductivity around 10^{-7} S/cm.[1] LAGP and LATP possess acceptable ionic conductivity. The bulk conductivity of LATP can be as high as 10^{-3} S/cm at room temperature. However, the grain boundary conductivity of LATP is nearly two orders of magnitude lower than the grain conductivity, generally of the order of 10^{-5} S/cm.[13]

In order to improve the grain boundary ion transport properties and the total ionic conductivity, researchers have made great efforts. Different preparation methods have been

*Project supported by the National Key Research and Development Program of China (Grant No. 2016YFB0100100), the National Natural Science Foundation of China (Grant Nos. 52315206 and 51502334), Fund from Beijing Municipal Science & Technology Commission, China (Grant No. D171100005517001).

†Corresponding author. E-mail: hli@iphy.ac.cn

© 2018 Chinese Physical Society and IOP Publishing Ltd

tried, including sol–gel, solution methods, pechini synthesis, melt quench, hydrothermal synthesis, co-precipitation, and mechano-chemical. The heat treatment processes have been investigated, including cold sintering, dry pressing, low temperature pressing, and varying calcination conditions.[14–21] Doping has also been widely studied.[22–24] Most of the above methods have improved the total conductivity to some extent and can enhance the grain boundary ionic conductivity. However, the improvement is not very significant.

Another route is to introduce the second phase into the pure LATP to modify the boundary, such as the ion insulator $AlPO_4$, Al_2O_3, B_2O_3, MgO, Li_2O,[25–29] or high dielectric constant materials like $BaTiO_3$, $SrTiO_3$,[28] and some poor lithium ion conductors with relative low melting point like Li_2CO_3, Li_3PO_4 as the sintering agent.[30] These modifications do improve the grain boundary conductivity and increase the total conductivity, which could be caused by high compactness or high carrier concentration in the grain boundary. However, the effect is still not very significant. It is found that the LATP/LAGP bi-layer electrolyte or LLTO/LATP composite electrolyte received significant effect on improving the total conductivity,[31,32] but the enhancement mechanism is not very clear and requires further investigation by using impedance spectra at a wide temperature range.[13]

Inspired by the previous efforts, in this paper, a similar but not well studied strategy is introduced. The LAGP is chosen as the second phase for the LATP due to its high grain boundary conductivity of 10^{-4} S/cm. It is almost one order of magnitude higher than that of the LATP. The main contents in this paper include: 1) solid state synthesis of the pure phase LAGP and LATP, 2) solid state synthesis of a series of composite electrolytes with LATP and LAGP by adjusting the weight ratio of the two electrolytes, 3) preparation and optimization of the ceramic sheets, 4) measurements of variable temperature AC impedance spectroscopy, 5) detailed data analysis and quantitative conclusion.

2. Experimental details

2.1. Synthesis of $Li_{1.5}Al_{0.5}Ge_{1.5}(PO_4)_3$ and $Li_{1.4}Al_{0.4}Ti_{1.6}(PO_4)_3$

The aluminum doped $Li_{1.5}Al_{0.5}Ge_{1.5}(PO_4)_3$ (LAGP) was prepared through solid state reaction. The stoichiometric mixtures of GeO_2, $(NH_4)_2HPO_4$, Li_2CO_3, and Al_2O_3 were mixed for 1 hour in an agate mortar. The mixtures were then heated at 400 °C for 2 hours with a heating rate of 2 °C/min in air to release the volatile products. The heated mixtures were ball-milled for 8 hours and then pressed into pellets in a stainless steel die and sintered at 900 °C for 3 hours with a heating rate of 2 °C/min in air.

The aluminum doped $Li_{1.4}Al_{0.4}Ti_{1.6}(PO_4)_3$ (LATP) was prepared similarly like preparing the LAGP. The differences lie in the original materials and the sintering process. The stoichiometric mixtures of TiO_2, $NH_4H_2PO_4$, Li_2CO_3, and Al_2O_3 were mixed for 1 hour in an agate mortar. The mixtures were then heated at 90 °C with a heating rate of 1 °C/min, then heated to 200 °C with a heating rate of 0.5 °C/min, finally heated to 400 °C with a heating rate of 0.5 °C/min to release the volatile products. The heated mixtures were ball-milled for 8 hours and then pressed into pellets in a stainless steel die and sintered at 900 °C for 5 hours with a heating rate of 2 °C/min in air.

After synthesizing the pure phase LAGP and LATP, the powders of LAGP and LATP and a series of composite electrolytes with different LATP/LAGP weight ratios (labeled as pure LATP, 80:20, 50:50, 20:80, and pure LAGP) were pressed into sheets with a diameter of 10 mm and sintered at different temperatures from 750 °C to 950 °C with a 50 °C interval for 3 hours under a heating rate of 2 °C/min in air.

2.2. XRD

The phase purity of the LAGP and LATP powders as well as the composite electrolytes that were sintered at 900 °C was examined at room temperature using a Bruker D8 Advance diffractometer with Cu-$K\alpha$ radiation and a LYNXEYE detector. Data was taken in the range of 10°–60° with 0.02° per step and a count time of 0.2 s at each step.

2.3. AC impedance spectroscopy

AC impedance measurement was carried out using a NOVO control analyzer. The gold was sputtered on both sides of the ceramic sheet as the block electrodes. The testing frequency range was from 1 Hz to 10 MHz and the temperature range was from 233 K to 293 K with a step of 10 K. The temperature was held for 30 min before each measurement.

3. Results and discussion

The XRD patterns of $Li_{1.5}Al_{0.5}Ge_{1.5}(PO_4)_3$ and $Li_{1.4}Al_{0.4}Ti_{1.6}(PO_4)_3$ are presented in Fig. 1. Both of the LAGP and LATP are pure phase and can be indexed to the *R*-3*C* space group, which is similar to the previous work.[13] No impurity phase is found in the XRD patterns. A slight peak shift toward the high angle direction is noticed in the LATP patterns compared to the $LiTi_2(PO_4)_3$ pattern, which is due to the smaller ion radius of Al^{3+} ($\sim$ 0.535 Å) compared with that of Ti^{4+} ($\sim$ 0.605 Å). No significant peak shift is found in the LAGP pattern compared with the $LiGe_2(PO_4)_3$ pattern due to the similar ion radius of Al^{3+} ($\sim$ 0.535 Å) and Ge^{4+} ($\sim$ 0.530 Å).

The impedance spectroscopy of LAGP and LATP measured at 233 K is shown as the Nyquist plot in Fig. 2. From Fig. 2, it can be seen that both the Nyquist plots of LAGP and

LATP consist of two semicircles, which appear at the high frequency and middle frequency, respectively. According to the previous literature results, the high frequency semicircle corresponds to the bulk impedance with the capacitance around 10^{-11} F and the middle frequency semicircle corresponds to the grain boundary impedance with the capacitance around 10^{-9} F.[33] Besides, it is easy to see that LAGP has similar apparent resistivity for the bulk and the grain boundary, while LATP has about two orders of magnitude difference in the resistivity between the bulk and the grain boundary, which is similar to the previous results.[13] Therefore, the existence of large grain boundary resistance of LATP significantly lowers the total conductivity.

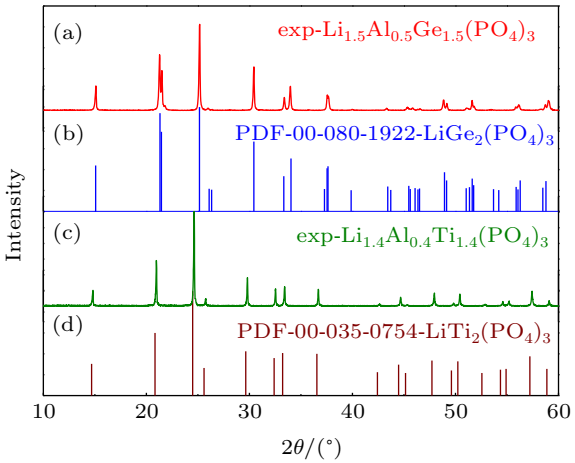


Fig. 1. (color online) XRD patterns of (a) $Li_{1.5}Al_{0.5}Ge_{1.5}(PO_4)_3$ and (c) $Li_{1.4}Al_{0.4}Ti_{1.6}(PO_4)_3$, PDF cards for (b) $LiGe_2(PO_4)_3$ and (d) PDF card $LiTi_2(PO_4)_3$.

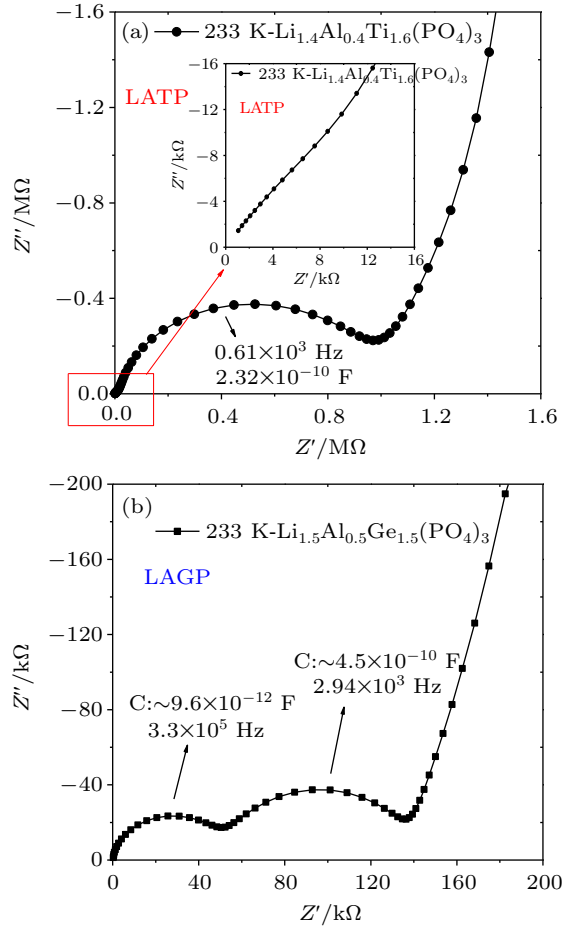


Fig. 2. (color online) Impedance data presented in Nyquist plot for (a) $Li_{1.5}Al_{0.5}Ge_{1.5}(PO_4)_3$ and (b) $Li_{1.4}Al_{0.4}Ti_{1.6}(PO_4)_3$ sintered at 900 °C for 3 hours.

Figure 3 shows the relationship of the compactness and grain boundary conductivity with the sintering temperature for the LAGP ceramic sheet. The compactness displayed in Fig. 3 is calculated according to the mass and geometry parameters of the ceramic sheet and the apparent grain boundary conductivity is calculated according to the following equation:

$$\sigma = \frac{1}{R}\frac{d}{A}, \tag{1}$$

where R is the grain boundary response impedance, d is the thickness of the ceramic sheet, and A represents the area of the ceramic sheet.

From Fig. 3, it can be inferred that the grain boundary conductivity is simultaneously changed with the compactness and achieves the highest value at 900 °C, then slightly decreases at 950 °C, which may be caused by the simultaneous variation in the compactness. Therefore, the samples sintered at 900 °C are selected to carry out further variable temperature AC impedance spectroscopy.

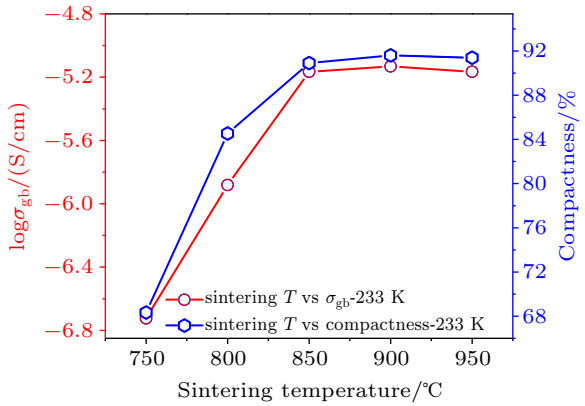


Fig. 3. (color online) Relationship of relative density and apparent grain boundary conductivity of $Li_{1.5}Al_{0.5}Ge_{1.5}(PO_4)_3$ with the sintering temperature.

Figure 4 demonstrates the Arrhenius plot and activation energy of the composite electrolytes. Figures 4(a)–4(e) represent the Arrhenius plots of different electrolytes labeled as LATP, 80:20, 50:50, 20:80, and LAGP, respectively. From Fig. 4(a), it can be inferred that pure LATP has an enormous difference in the conductivity between the bulk and the grain boundary under varying temperature, while the pure LAGP has similar bulk and grain boundary conductivity. However, with the increasing weight ratio of LAGP to LATP, the difference between the bulk and the grain boundary becomes smaller, which can be inferred from Figs. 4(b)–4(d) and this result indicates that the composite electrolytes 80:20, 50:50,

and 20:80 may benefit from the high bulk conductivity of LATP and the high grain boundary conductivity of LAGP.

Figure 4(f) presents the activation energy of the composite electrolytes. The hollow dot in Fig. 4(f) represents the experiment data while the dashed line is the simulation results, which is calculated according to the following equation:

$$E_{\mathrm{aCal}}=E_{\mathrm{aLATP}}x+E_{\mathrm{aLAGP}}(1-x), \tag{2}$$

where E_{aCal} stands for the calculated activation energy, E_{aLATP} is the activation energy of pure LATP, and E_{aLAGP} represents the activation energy of pure LAGP, x is the volume ratio of LATP in the composite electrolytes, which can be roughly calculated according to the mass ratio and density of LATP in the composite electrolytes. From Fig. 4(f), it can be seen that the bulk activation energy of the composite electrolytes is closely related to the weight ratio of LAGP and shows a linear variation trend with the LATP volume ratio.

Figure 5 shows the relationship of the ionic conductivity with the LATP weight ratio and test temperature. Figure 5(a) illustrates the variation trend of the total conductivity with the LATP weight ratio and test temperature, while figures 5(b) and 5(c) correspond to the bulk and the grain boundary. The composite electrolyte 20:80 has higher total conductivity than pure LAGP and LATP as shown in Fig. 5(a), which is about two to three times higher than the pure LAGP and over six times higher than the LATP. From Fig. 5(b), it can be seen that with

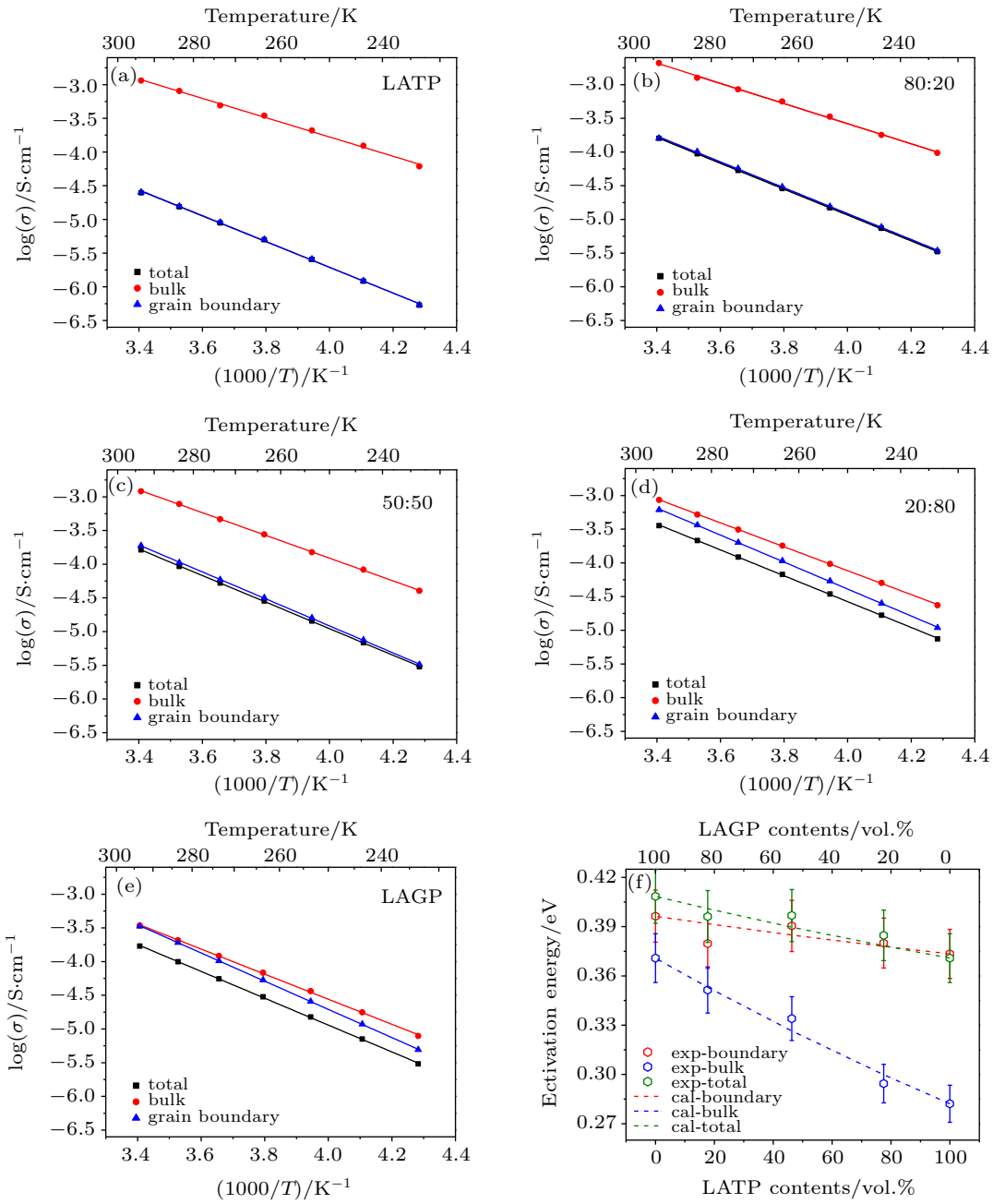


Fig. 4. (color online) The Arrhenius plots and activation energy of different composite samples: (a) pure $Li_{1.4}Al_{0.4}Ti_{1.6}(PO_4)_3$, (b) 80:20, (c) 50:50, (d) 20:80, (e) pure $Li_{1.5}Al_{0.5}Ge_{1.5}(PO_4)_3$; (f) activation energy for different electrical regions of different samples.

the increase of the LATP weight ratio, the bulk conductivity is simultaneously increased and the highest bulk conductivity appears at the LATP/LAGP weight ratio of 80:20, which is higher than the bulk conductivity of pure LATP. Figure 5(c) displays a contrary variation trend, with the increase of the LAGP weight ratio, the grain boundary conductivity is simultaneous increased and the highest grain boundary conductivity appears at the LATP/LAGP weight ratio of 20:80, which is higher than the grain boundary conductivity of pure LAGP.

Combining the results of Figs. 5(b) and 5(c), it can be inferred that the composite electrolytes 80:20, 50:50, and 20:80 may take advantage of the high bulk conductivity of LATP and the high grain boundary conductivity of LAGP. However, the electrolyte 80:20 has higher bulk conductivity than pure LATP, which is difficult to understand if the composite electrolytes were the mixture of LATP and LAGP and no interaction around the interface of LATP and LAGP occurred during the sintering process.

Suppose that the composite electrolytes consists of electrolyte A and electrolyte B with different intrinsic bulk conductivities σ_A and σ_B, the volume ratio or weight ratio of electrolyte A is x $(0 \leq x \leq 1)$, to simplify the discussion, the total bulk conductivity can be expressed as the following equation without considering the interaction between A and B:

$$\sigma_{\text{bulk}} = \sigma_A x + \sigma_B (1 - x). \tag{3}$$

According to Eq. (3), the total bulk conductivity could not be larger than the maximum one of the two electrolytes, which is inconsistent with the experiment results displayed in Fig. 5. Therefore, there must be other factors that enhance the bulk conductivity of the composite electrolytes. A similar situation occurs for the grain boundary conductivity.

Figure 6 displays the bode plot of the composite electrolytes measured at 233 K, which shows the relation of the response frequency with the tangent value of phase angle and conductivity. Figure 6(a) shows two typical response frequencies for each composite electrolyte, which appear at high

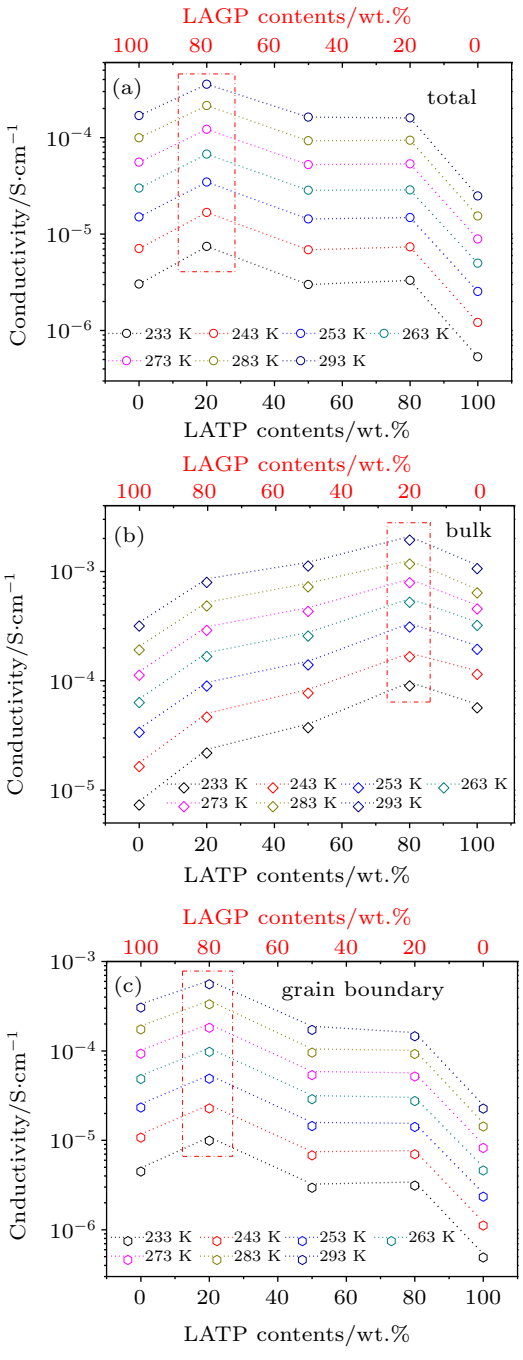


Fig. 5. (color online) Conductivity of different electrical regions in the composite samples at different temperatures: (a) total conductivity, (b) bulk conductivity, (c) grain boundary conductivity.

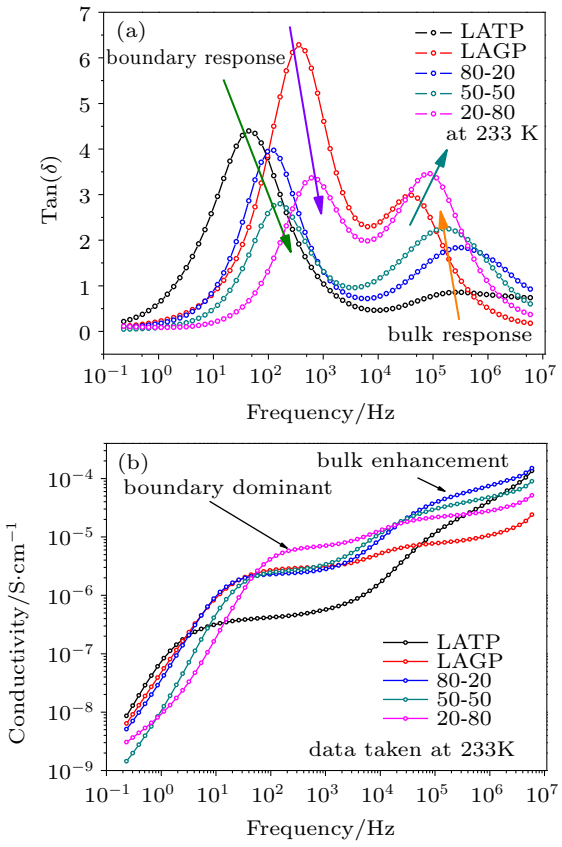


Fig. 6. (color online) (a) Relationship of response frequency with response angle for different composite electrolytes and (b) relationship of conductivity with response frequency.

frequency region and middle frequency region, respectively. According to the previous literature results,[33] the bulk response appears at the high frequency region and the grain boundary response occurs at the middle frequency region. The inner relationship can be explained by the following equation:[33]

$$\omega RC = 1, \tag{4}$$

$$\tau = RC, \tag{5}$$

where R is the response impedance, C is the capacitance, ω is the circular frequency that equals to $2\pi f$, and τ is the characteristic relaxation time constant, which is closely related to the ion transport properties. The electrolyte 80:20 possesses the highest bulk response frequency as illuminated in Fig. 6(a), while the electrolyte 20:80 has the highest grain boundary response frequency, which corresponds to the minimum characteristic relaxation time constant. These results are consistent with the enhanced bulk and grain boundary conductivity in electrolytes 80:20 and 20:80 as illustrated in Figs. 5(b) and 5(c). A similar variation trend of the conductivity is demonstrated in Fig. 6(b).

Figures 7(a)–7(c) display the Nyquist plot of LAGP measured at 233 K and figure 7(d) shows the relationship of the bulk and grain boundary conductivity with the ratio of C_{gb} to C_{bulk}. Figures 7(a)–7(c) indicate that the bulk response capacitance C_{bulk} changes slightly with a typical value around 4.5×10^{-11} F under the varying sintering temperature, while the grain boundary response capacitance changes about three times from 8.7×10^{-10} F to 2.7×10^{-9} F. Both the bulk and the grain boundary capacitances can be calculated according to the following equation:

$$C = \varepsilon_r \varepsilon_0 \frac{A}{d}, \tag{6}$$

where A is the area of the ceramic sheet, d is the effective thickness for the bulk or the grain boundary, ε_r and ε_0 represent the relative dielectric constant and vacuum dielectric constant, which are not sensitive to the temperature as illustrated in Fig. 8.

Figures 7(a)–7(c) show that only a slight variation occurs to the bulk capacitance as well as to the bulk conductivity under different sintering temperature, which means that the geometry parameters A and d do not change significantly and the bulk conductivity is not sensitive to the compactness, even the compactness of the ceramic varies from 65% to 91% as illustrated in Fig. 3. However, the grain boundary capacitance changes greatly with the sintering temperature, as it can be seen from Eq. (6) that the capacitance is mainly influenced by the geometry parameters A, d and the dielectric constant ε_r,

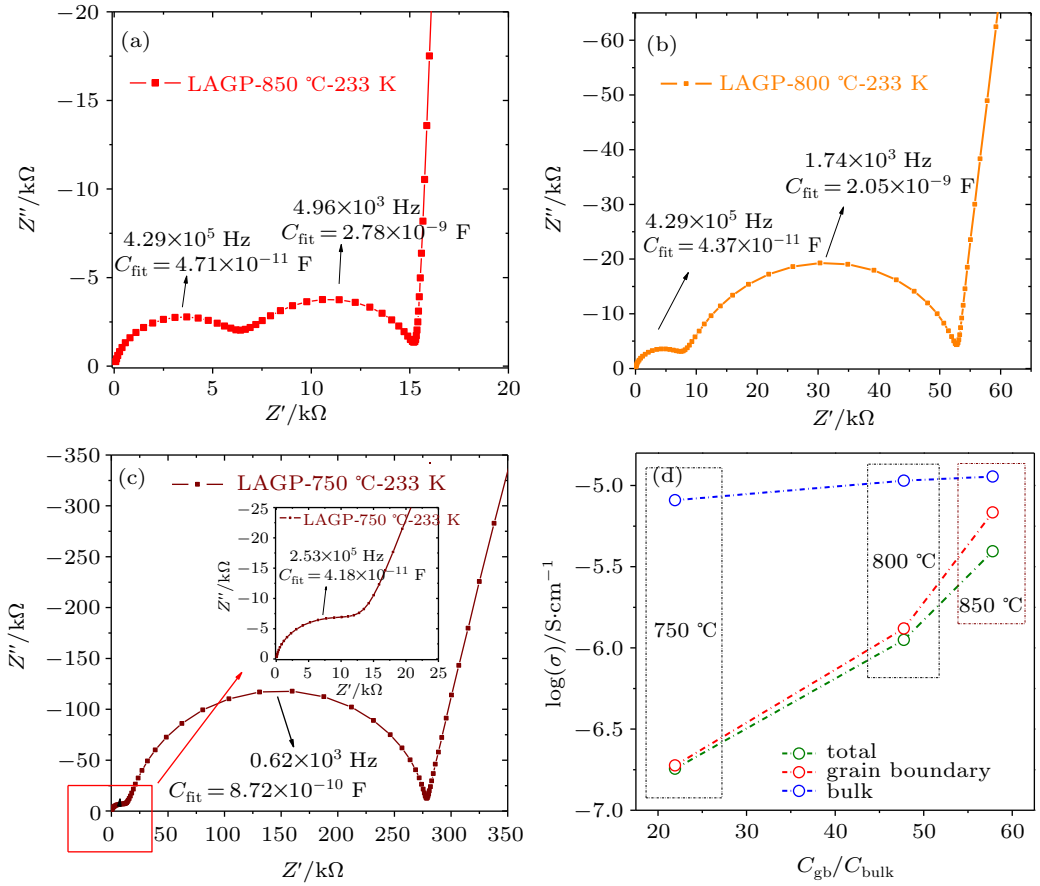


Fig. 7. (color online) (a) Impedance data for $Li_{1.5}Al_{0.5}Ge_{1.5}(PO_4)_3$ at 233 K under different sintering temperature and (b) the relation of the bulk and grain boundary conductivity with the ratio of C_{gb}/C_{bulk}.

both the apparent geometry area A and the dielectric constant ε_r are kept as a constant, therefore, the increased capacitance of the grain boundary should be due to the decreased grain boundary thickness, which induces the decrease of the grain boundary resistance. The absolute variation of the grain boundary thickness can be measured with the ratio C_{gb}/C_{bulk}.

Figure 8 shows the relationship of the grain boundary response capacitance with the measuring temperature. The grain boundary capacitance is nearly constant with the variation temperature as shown in Fig. 8(a). However, a huge difference in the grain boundary capacitance among the composite electrolytes is observed in Fig. 8(b). The composite electrolytes 80:20, 50:50, and 20:80 have larger grain boundary capacitance than the pure LATP and LAGP. According to Eq. (6), the capacitance is closely related to the geometry parameters A, d and the dielectric constant ε_r. From Table 1, it is easy to see that the ratio A/d is nearly the same among the composite electrolytes, but the capacitance between different composite electrolytes changes by more than two times, which means that the dielectric constant ε_r of electrolytes 80:20, 50:50, and 20:80 may be different from that of LAGP and LATP. As it is known that the dielectric constant is mainly determined by the atomic properties of the electrolyte, the great variation in the dielectric constant in the electrolytes 80:20, 50:50, and 20:80 means that both the bulk and the grain boundary properties are different from those of LAGP and LATP. The interaction is significant in the composite electrolytes during the sintering process.

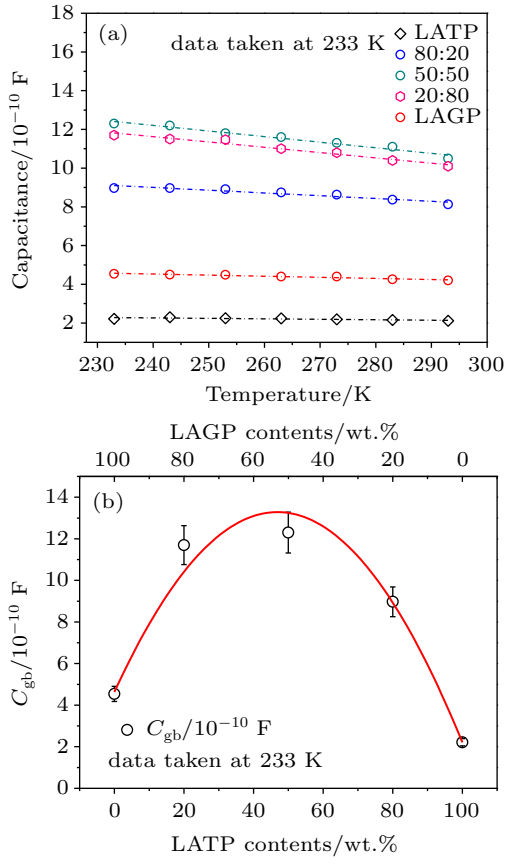


Fig. 8. (color online) (a) Grain boundary capacitance of different composite samples and (b) the relationship of grain boundary capacitance with ratio of LATP to LAGP.

In fact, the grain boundary conductivity is closely related to the compactness of the ceramic sheet, which has been reported in the previous study.[13] According to Table 1, the electrolytes 80:20, 50:50, and 20:80 have lower shrinkage in radial direction, which means relatively low densities of these samples. However, higher bulk conductivity and grain boundary conductivity are observed compared to the original LAGP and LATP, which means that the enhancement is not due to the compactness and shall be due to the interfacial interaction or the variation of atomic structure.

Table 1. Geometry parameters of the composite electrolytes.

Sample	d/cm	D/cm	Area/cm^2	(A/d)/cm	Shrinkage/%
LATP	0.323	0.882	0.61	1.89	11.8
80–20	0.286	0.924	0.67	2.34	7.6
50–50	0.288	0.920	0.66	2.30	8
20–80	0.244	0.872	0.60	2.46	12.8
LAGP	0.241	0.852	0.57	2.37	14.8

For the bulk conductivity enhancement mechanism, which has been discussed in the above paragraph, the compactness has very little impact on the accurate measuring of the bulk conductivity, as illustrated in Fig. 7(d). However, the electrolyte 80:20 has higher bulk conductivity than the pure LATP, which could not be interpreted with Eq. (3). As the bulk conductivity is an intrinsic variable and mainly influenced by the crystal structure, this means that the crystal structure of the electrolyte 80:20 should be different from that of pure LATP and LAGP, such as the lattice parameters or the carrier concentration. To further discuss the enhancement of the ionic conductivity, detailed structure information of the composite electrolytes is necessary.

The XRD patterns of the composite electrolytes sintered at 900 °C for 3 hours are displayed in Fig. 9(a) from 10° to 60°. Figures 9(b) and 9(c) demonstrate the local zoom-in images of Fig. 9(a). From Fig. 9(b), it can be clearly seen that with the increased LAGP weight ratio in the composite electrolytes, the peak around 21.2° shifts toward the high angle direction continuously, which is due to the larger lattice parameters of LATP than those of LAGP. Figure 9(c) shows that only the electrolyte 80:20 is pure phase with similar crystal structure as the original LATP. The chemical formula of electrolyte 80:20 can be expressed as $Li_{1.42}Al_{0.42}Ge_{0.3}Ti_{1.28}(PO_4)_3$, with small lattice parameters and large lithium ion concentration come wide lithium ion pathway and carrier concentration, which finally induce higher bulk conductivity. The electrolytes 50:50 and 20:80 are not single phase which consist of little LATP phase and some $Li_{1+x}Al_xGe_yTi_{2-x-y}(PO_4)_3$ solid solution phase that may have very high grain boundary conductivity. Therefore,

the enhanced bulk conductivity shall be due to the solid solution phase of $Li_{1.42}Al_{0.42}Ge_{0.3}Ti_{1.28}(PO_4)_3$ and the enhanced grain boundary conductivity may be due to the excellent interfacial phase between $Li_{1+x}Al_xGe_yTi_{2-x-y}(PO_4)_3$/LATP, which can acquire high grain boundary conductivity at a relative low compactness.

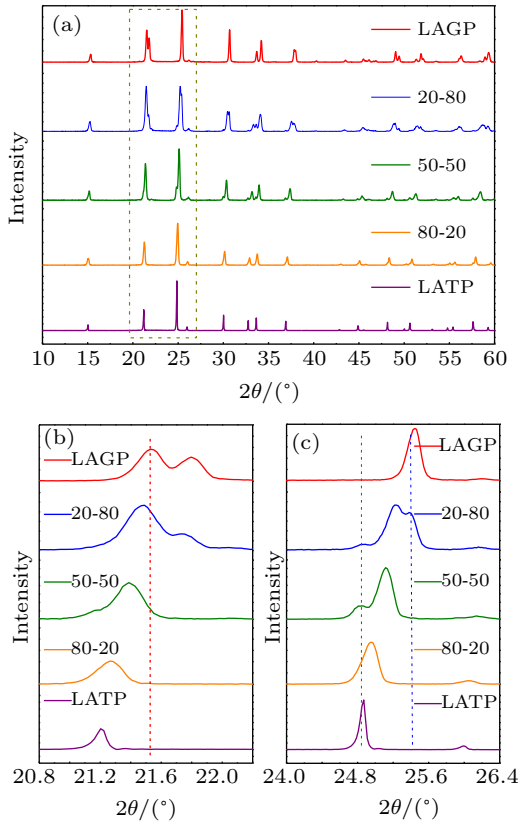


Fig. 9. (color online) XRD patterns of samples with different LATP/LAGP weight ratios, (a) full region XRD patterns, (b) local zoom-in image, (c) local zoom-in image.

4. Conclusion

Pure phase LAGP and LATP were synthesized through solid reaction and a series of composite electrolytes consisted of LAGP and LATP with different weight ratios were designed. Systematic variable temperature AC impedance spectra were investigated to clarify the ion transport properties of the composite electrolytes. The results indicate that the composite electrolyte with the LATP/LAGP weight ratio of 80:20 has the highest bulk conductivity, which may be due to the solid solution phase of $Li_{1.42}Al_{0.42}Ge_{0.3}Ti_{1.28}(PO_4)_3$, while the highest grain boundary conductivity appears at the LATP/LAGP weight ratio of 20:80 and this shall be due to the excellent interfacial phase between $Li_{1+x}Al_xGe_yTi_{2-x-y}(PO_4)_3$/LATP, which can acquire high grain boundary conductivity at a relatively low compactness. All the composite electrolytes have higher total conductivity than the pure LAGP and LATP, which highlights the importance of fine tuning the heterogeneous interface on designing a composite fast ionic conductor. Finally, to further comprehend the micro mechanism of the enhanced ionic conductivity at the interface, future research work is on the way to reveal the interfacial structure from the atomic level.

References

[1] Marcinek M, Syzdek J, Marczewski M, Piszcz M, Niedzicki L, Kalita M, Plewa-Marczewska A, Bitner A, Wieczorek P, Trzeciak T, Kasprzyk M, Łężak P, Żukowska Z, Zalewska A and Wieczorek W 2015 *Solid State Ionics* **276** 107

[2] Yao X, Huang B, Yin J, Peng G, Huang Z, Gao C, Liu D and Xu X 2016 *Chin. Phys. B* **25** 018802

[3] Meyer W H 1998 *Adv. Mater.* **10** 439

[4] Gao J, Zhao Y S, Shi S Q and Li H 2016 *Chin. Phys. B* **25** 018211

[5] Kato Y, Hori S, Saito T, Suzuki K, Hirayama M, Mitsui A, Yonemura M, Iba H and Kanno R 2016 *Nature Energy* **1** 16030

[6] Murugan R, Thangadurai V and Weppner W 2007 *Angewandte Chemie* **46** 7778

[7] Yoshiyuki Inaguma, Chen L Q, Itoh M, Nakamura T, Uchida T, Ikuta H and Wakihara M 1993 *Solid State Commun.* **86** 689

[8] Fujimura K, Seko A, Koyama Y, Kuwabara A, Kishida I, Shitara K, Fisher C A J, Moriwake H and Tanaka I 2013 *Advanced Energy Materials* **3** 980

[9] Yamamoto H and Nakamura O 1997 *Journal of Power Sources* **68** 397

[10] Knauth P 2009 *Solid State Ionics* **180** 911

[11] Aono H, Sugimoto E, Sadaoka Y, Imanaka N and Adachi Gin-ya 1990 *J. Electrochem. Soc.* **137** 1023

[12] Xu X, Wen Z, Wu X, Yang X and Gu Z 2007 *Journal of the American Ceramic Society* **90** 2802

[13] Wang S, Ben L, Li H and Chen L 2014 *Solid State Ionics* **268** 110

[14] Schell K G, Bucharsky E C, Lemke F and Hoffmann M J 2017 *Ionics* **23** 821

[15] Zhao E, Ma F, Jin Y and Kanamura K 2016 *J. Alloy. Compd.* **680** 646

[16] Ma F, Zhao E, Zhu S, Yan W, Sun D, Jin Y and Nan C 2016 *Solid State Ionics* **295** 7

[17] Liu X G, Fu J and Zhang C H 2016 *Nanoscale Research Letters* **11** 551

[18] Yan B, Zhu Y, Pan F, Liu J and Lu L 2015 *Solid State Ionics* **278** 65

[19] Kim K M, Shin D O and Lee Y G 2015 *Electrochimica Acta* **176** 1364

[20] Morimoto H, Hirukawa M, Matsumoto A, Kurahayashi T, Ito N and Tobishima S I 2014 *Electrochemistry* **82** 870

[21] Kotobuki M, Kobayashi B, Koishi M, Mizushima T and Kakuta N 2014 *Materials Technology* **29** A93

[22] Kothari D H and Kanchan D K 2016 *Physica B* **494** 20

[23] Kothari D H and Kanchan D K 2016 *Physica B* **501** 90

[24] Arbi K, Bucheli W, Jimenez R and Sanz J 2015 *Journal of the European Ceramic Society* **35** 1477

[25] Jadhav H S, Kalubarme R S, Jang S Y, Jung K N, Shin K H and Park C J 2014 *Dalton Transactions* **43** 11723

[26] Chung H and Kang B 2014 *Solid State Ionics* **263** 125

[27] Jadhav H S, Cho M S, Kalubarme R S, Lee J S, Jung K N, Shin K H and Park C J 2013 *Journal of Power Sources* **241** 502

[28] Thokchom J S and Kumar B 2008 *Journal of Power Sources* **185** 480

[29] Leo C J, Rao G V S and Chowdari B V R 2003 *Solid State Ionics* **159** 357

[30] Yu S C, Mertens A, Gao X, Gunduz D C, Schierholz R, Benning S, Hausen F, Mertens J, Kungl H, Tempel H and Eichel R A 2016 *Functional Materials Letters* **9** 1650066

[31] Zhao E, Ma F, Guo Y and Jin Y 2016 *Rsc Advances* **6** 92579

[32] Onishi H, Takai S, Yabutsuka T and Yao T 2016 *Electrochemistry* **84** 967

[33] Irvine J T S, Sinclair D C and West A R 1990 *Advanced Materials* **2** 132